World Applied Sciences Journal 31 (11): 1952-1959, 2014
ISSN 1818-4952

DOI: 10.5829/idosi.wasj.2014.31.11.21587

Content Based Image Retrieval Using Improved Radon Transform under Various Queries

[1]S. Singaravelan and [2]D. Murugan

[1]Department of Computer Science and Engineering,
PSR Engineering College, Sivakasi, Tamilnadu, India
[2]Department of Computer Science and Engineering,
Manonmaniam Sundaranar University, Tirunelveli, Tamilnadu, India

Abstract: Image Retrieval is very one of the biggest task in the recent years. It is widely used in many real time databases to retrieve related images in various fields like medical, military, online shopping etc. This paper offers with using radon transform followed by PCA and LDA techniques for image retrieval is called as Combined Radon Space Features Set (CRSFS). Caltech 101 database image sets used in this paper. The radon transform used in FFT based slice theorem. The correct direction is select means the computation time and complexity of operation is less to achieve good retrieval rate. Here PCA is used to reduce the dimensionality in feature vectors produced by radon transform and LDA is used to find the set of basic vectors which maximizes the radio between-class scatter and within-class scatter. In order to verify our method to various data set in different condition like rotation, scaled and noisy query environments like additive, Gaussian, salt and pepper. And our proposed method was achieving better retrieval rate.

Key words: Image Retrieval (IR) · Combined Radon Space Features Set (CRSFS) · Radon Transform (RT) · Fast Fourier Transform (FFT) · Principal Component Analysis (PCA) · Linear Discriminant Analysis (LDA) · Noise Reduction

INTRODUCTION

Content based image retrieval (CBIR) is a one of the popular techniques which is visual contents to search and browsing digital images from image databases according to user's interests [1-22]. The CBIR systems is used many real time applications and databases in medical, military, human identification & security systems and online searching & shopping [23]. The term 'content based' means the actual contents of the image rather than keywords, tags or descriptions associated with the image. The CBIR classified in two ways first one is text based retrieval and second one in content based retrieval. In our proposed method mainly concentrate in content based image retrieval. The two mode of CBIR is analyzed first one is low level features like color, shape and texture value to classified and retrieved the images. Low level features future classified in to two ways like global features and local features. Global features mean its measure the color, shape and texture information on entire image. Local features mean its measure the color, shape and texture information on some specific region and condition based to analyze the image [1].

Existing Work: Ho young [2] is used spatial color descriptor for image retrieval and video segmentation using the color histogram and angle histogram and spatial distribution of color pairs at color edges in an image. The error rate is 28.6%. The classical image database used it contains 5000 images.

Gwenole [3] is introduced adaptive non separable wavelet transform to CBIR its extracted image signature is derived from this new method. The error rate is 4.6%. The medical database DRD, DDSM & nonmedical database FD,VisTex is used.

Corresponding Author: S. Singaravelan, Department of Computer Science and Engineering,
PSR Engineering College, Sivakasi, Tamilnadu, India.

Manesh kokare [4] is used new rotated complex wavelet filters to measure the texture values based on image retrieval. The error rate is 17.2%. The texture image database like Brodatz and VisTex is used.

Hui hui [5] is proposed a novel techniques for object spatial relationships semantic extraction and low level features extraction values was integrated. The error rate is 8.3%. The classical image database used.

Te –wei [6] is used multi resolution wavelet features of interest is apply to CBIR in discrete wavelet transform. The error rate is 23.7%. The classical image database used it contains 1000 images.

Gwenole [7] is integrated to proposed estimate query image in two function wavelet basic and regression function. The error rate is 3.1%. The Caltech 101, MOSSIDOR, face database and VisTex database used.

Yue Gao [8] is proposed an approach that simultaneously utilize both visual and textual information to estimate the relevance of user tagged images using hupergraph learning approach. The error rate is 2.4%. The Flicker datasets used it contains 104,000 images and 83,999 unique tags is used.

Qianni [9] is used to automatically combine heterogeneous visual features for histology image retrieval. The approach is multi objective learning methods. The error rate is 24%. The BiMed image database used it contains 20000 images.

Kekre [10] is proposed innovative idea of sectorization of full haar wavelet transformed images for extracting features. The paper proposed two phases to sector the image plane is forward and backward plane. The error rate is 24%. The classical image databases used.

Yi-chen [11] is using radon transform to examine in-plane rotation and scale invariant clustering in cbir objects. The error rate is 6.4%. The Smithsonian isolated leaf and Kimia - shape based database & Brodatz - texture based database used.

Proposed Method: The method used in this paper for content based image retrieval if Fig (1). It has a query phase and another one is data/database registered phase. In the data/database registered phase the set of images are transformed in to radon space using radon transform. Here radon transform performed based on 2D-FFT slice theorem is applied in this method. The data generated by radon transform are reduced using principal component analysis (PCA). From those reduced dataset (ie. the mainly valuable components) a set of basic vector which maximize the radio between-class scatter and within-class scatter using linear discriminant analysis(LDA). One basic

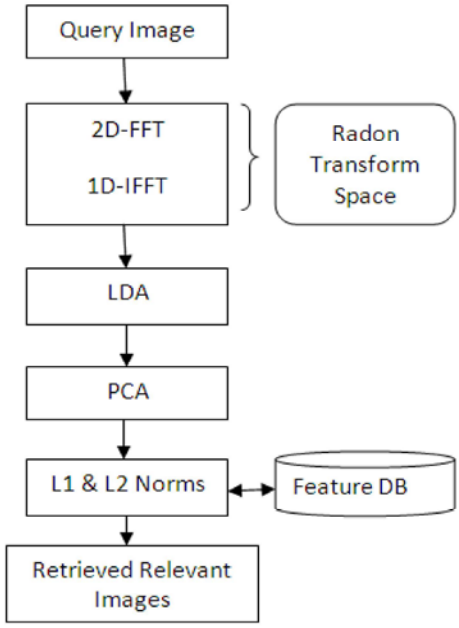

Fig. 1: Proposed CBIR Method

vector for each image is derived and stored in the database. So for image database there are set of basic vectors are stored regardless of the number of images used for each dataset in the training set. The length of the basic vector depends on the number of components selected by the PCA stage. The query phase the input image is transformed into the radon space using radon transform based on 2D-FFT slice theorem. The PCA reduction is carried out as same as in the data/database registered phase. The resultant vector is calculated using distance measure comparison methods was used to check the query phase weight vector values W was compared to data/database registration phase weight vectors values. The most similar weight vectors values images are listed in retrieval results. In this work two types of distance measure used, L1 Norm and L2 Norm. L1 Norm measures the absolute distance between the pixels of the original and the corrected image. L2 Norm measures the Euclidian distance between the pixels of the original and the corrected image. The method which is stated in this paper was evaluated using the Caltech 101 database datasets which contains classical images & texture images. There are 8 different datasets used in this work. The images are color with a resolution of 120x120. For some of the datasets, the image were taken at different angle, scaling and noise added and apply for our experiments. The subsequent part discussion of each main part of the method process is presented.

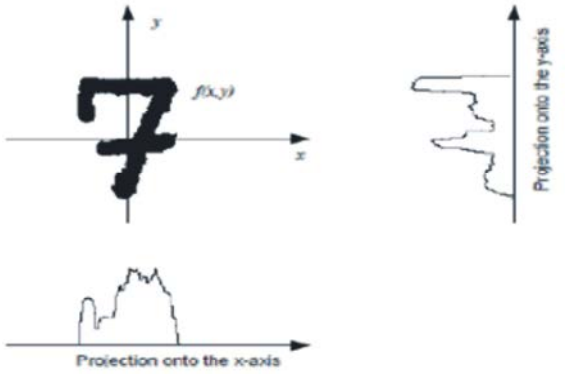

Fig. 2: Radon Transform Horizontal & Vertical Projection View

Radon Transform: The radon transform is used many applications like categories the visual objects [12], rotation invariants in objects identification [13, 15], face recognitions [14], image recognitions [16]. The radon transform is the projection of the image intensity along a radial line oriented at a specific angle. The radial coordinates are the values along the x'-axis, which is oriented at □ degree counter clockwise from the x-axis. The origin of the both axis is the center pixel of the image. Radon transform of an image representation as a matrix, called sinogram.

Horizontal and Vertical Projection: The popular form expresses lines is

$$t = x * \cos(\theta) + y * \sin(\theta) \tag{1}$$

θ – angle & t – smallest distance to the origin of the coordinate system

Projection can be computed along any angle θ, by use general equation of the radon transform

$$g(t,\theta) = \iint_{-\infty}^{+\infty} f(x,y)\delta(t - x(\cos(\theta) - y\sin(\theta))dxdy \tag{2}$$

The very strong property of the radon transform is the ability to extract lines (curves in general) from very noisy images.

Rotation Invariance: The radon transform of a two variable function x is defined as

$$R_\theta x(t) = \int_{-\infty}^{\infty} x(t\cos\theta - s\sin\theta, t\sin\theta + s\cos\theta)ds \tag{3}$$

$$where (t,\theta) \in (-\infty,\infty)\times(0,\pi) \quad \forall s \quad \in R$$

To compute the value at any given point (t,□) in the radon domain by integrating along the line:

$$(u,v) = (t\cos\theta - s\sin\theta + s\cos\theta) \tag{4}$$

If x‘ is a rotated copy of x by on angle θ
Simple proof shows $R_\theta \bar{x}(t) = R_{\theta+\hat{\theta}} x(t) \ \forall t,\theta$

Let $\sigma_\theta \underline{\Delta} Var_t[R_\theta x(t)]$ denotes the variance with respect to t of the RT at θ.
σ_θ - Useful in estimating the principal orientation in an image.

Estimate $\hat{\theta}$

$$\hat{\theta} = \arg\min_\theta \left(\frac{d^2\sigma\theta}{d\theta^2}\right) \tag{5}$$

Scale Invariance: Let x’ is the scaled copy of x with scaling factor ε such that

$$\bar{x}(u,v) = x(\xi u, \xi v) \tag{6}$$

Relate this to RT,

$$R_\theta \bar{x}(t) = \int_{-\infty}^{\infty} \bar{x}(t\cos\theta - s\sin\theta + s\cos\theta)ds$$

$$= \int_{-\infty}^{\infty} x(\xi t\cos\theta - \xi s\sin\theta, \xi t\sin\theta + \xi s\cos\theta)ds$$

$$= \frac{1}{\xi} R_\theta x(\xi t)$$

From this observation, scale invariance can be achieved through the normalization in the RT.

Principal Component Analysis (PCA): Principal Components Analysis (PCA) is one of several statistical tools available for reducing the dimensionality of a data set [19, 20 and 24]. Its relative simplicity and both computational and in terms of understanding what’s happening and make it a particularly popular tool. The major goal of principal components analysis is to reveal hidden structure in a data set. In so doing, we may be able to

- Identify how different variables work together to create the dynamics of the system

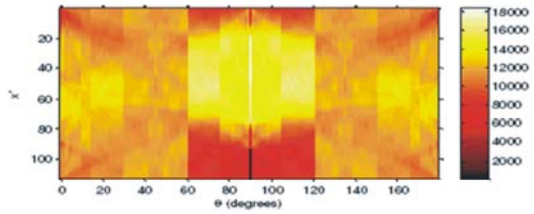

Fig. 4: FFT based Radon Transform Sinogram for an image

- Reduce the dimensionality of the data
- Decrease redundancy in the data
- Filter some of the noise in the data
- Compress the data

The training set D and testing set Q on basic vectors:

Step 1: Calculate mean value *m* for training set and subtract it from the training set

$$m = \frac{1}{n}\sum_{i=1}^{n} D_i \tag{7}$$

All training set $D_i = D_i - m$

Step 2: Calculate the eigenvectors and eigenvalues of the training set covariance matrix C_i

$$C_t = D \cdot D^Q \tag{8}$$

The eigenvectors corresponding N largest eigenvalues of C_i. These construct the principal component matrix (V).

Step 3: The basic vector matrix (E) is defined by:

$$E = V \cdot D^Q \tag{9}$$

Step 4: The reduced feature vectors for training and testing data calculated by:

$$WD = D \cdot E \tag{10}$$

$$W\,Q = Q\,.\,E \tag{11}$$

Linear Discriminant Analysis (LDA): The LDA is used to find the set of basic vectors which maximizes the radio between –class scatter and within-class scatter [19, 21, 22-24].

The between class scatter matrix is defined by:

$$S_B = \sum_{i=1}^{c} N_i (mi - mt)\,(mi - mt)^Q \tag{12}$$

Here, C – Classes, Ci- ith Class, Ni – number of samples, Mt – mean of the hole dataset, Mi – mean of the ith class.

The within- class scatter matrix is defined by:

$$S_W = \sum_{i=1}^{c}\sum mk \in ci\ \ (mk - mi)\,(mk - mi)^Q \tag{13}$$

The basic vector is defined by:

$$W = \arg\max\left(\frac{\left|W^Q S_B W\right|}{\left|W^Q S_W W\right|}\right) \tag{14}$$

Solving Equations (11) to produces a matrix W whose columns are the eigenvectors corresponding to the largest eigenvalues are calculated. These columns are the linear discriminant function related with classes as one of the function for each data. These functions are stored in the database to perform the classification.

Noises in Image: Image noise [17] is random (not present in the object imaged) variation of brightness or color information in images and is usually an aspect of electronic noise. It can be produced by the sensor and circuitry of a scanner or digital camera. Image noise can also originate in film grain and in the unavoidable shot noise of an ideal photon detector. Image noise is an undesirable by-product of image capture that adds spurious and extraneous information.

Fat-tail distributed or "impulsive" noise is sometimes called salt-and-pepper noise or spike noise. An image containing salt-and-pepper noise will have dark pixels in bright regions and bright pixels in dark regions. This type of noise can be caused by analog-to-digital converter errors, bit errors in transmission, etc. It can be mostly eliminated by using dark frame subtraction and interpolating around dark/bright pixels.

$$f(x) = \begin{cases} f_a \ for\ x = a \\ f_b \ for\ x = b \\ 0 \ otherwise \end{cases} \tag{15}$$

In this equation, if fa or fb is zero, we have unipolar impulse noise. If both are nonzero and almost equal, it is called salt-and-pepper noise. Impulsive noises can be

positive and / or negative. It is often very large and can go out of the range of the image. It appears as black and white dots, or saturated peaks.

Amplifier noise is a major part of the "read noise" of an image sensor, that is, of the constant noise level in dark areas of the image. In color cameras where more amplification is used in the blue color channel than in the green or red channel, there can be more noise in the blue channel

$$I_V(x,y) = I(x,y) + V(x,y) \tag{16}$$

where Iv is the observed image with noise, I is the true signal (image) and V is the noise component. Many additive noise models exist and the following are some common additive noise models with their Probability Density Function (PDF) [18]. Gaussian noise is most commonly used as additive white noise to yield additive white Gaussian noise.

$$f(x) = \frac{1}{\sqrt{2\pi\sigma^2}} e^{\frac{-(x-\mu)^2}{2\sigma^2}} \tag{17}$$

where the parameter μ is called the mean and it determines the location of the peak of the density function, parameter σ is called standard deviation and σ2 is variance of the distribution.

Uniform noise is not often encountered in real-world imaging systems, but provides a useful comparison with Gaussian noise. The PDF of uniform distribution is given by

$$f(x) = \begin{cases} \frac{1}{\sigma^2\sqrt{3}} & for\ |x| \le \sigma\sqrt{3} \\ 0 & else \end{cases} \tag{18}$$

Distance Measures:

L1& L2 Norm:

L2 Norm measures the Euclidian distance between the weight vector values of the query and the database images.

Formula for the L2 norm is:

W1 = ((img_query _(w) - img_database_(w))^2)

L1 Norm measures the absolute distance between the weight vector values of the queryl and the database images.

Formula for the L1 norm is:

W2= (abs (img_query _(w) - img_database_(w))

Performance Measure: In the CBIR performance measure is calculated in this work was universal methods Precision & Recall.

$$\text{Precision} = \frac{No\ of\ relevant\ images\ retrieved}{Total\ no\ of\ images\ retrieved}$$

$$\text{Recall} = \frac{No\ of\ relevant\ images\ retrieved}{Total\ no\ of\ images\ in\ the\ database}$$

Experiments: The proposed image retrieval method (CRSFS) was applied Caltech 101 database datasets images in the size 120x120 pixel resolution. Totally four experiments conducted. Each with different query environments like normal, rotated, scaled and noisy and performance was evaluated and represent in Tables (1, 2, 3, 4). The two types of distance measure function was used in our proposed method is L1 & L2 performance was evaluated and represent in Table (5). The proposed method overall performance was compared to other existing traditional methods in Fig 7.

Situation-1 : In this situation performance measured in different rotated angle in query image. It's applied in 8 datasets combined with classical & texture images. The selected Query rotated angles was 30°, 60°, 90° and 120°. See Table (1). It obtained percentage is around 97.8%.

Situation - 2: In this situation performance measured in different scaling factor in query image. It's applied in 8 datasets combined with classical & texture images. The selected Query scaling factor was 30x30, 60x60 and 120x120. See Table (2). It obtained percentage is around 98.3%.

Situation-3: In this situation performance measured in different noise information added to query image like salt & pepper, additive and uniform noise in query image. It's applied in 8 datasets combined with classical & texture images. See Table (3). It obtained percentage is around 98.5%.

Situation-4: In this situation performance measured in standard image used as query image. It's applied in 8 datasets combined with classical & texture images. See Table (4). It obtained percentage is around 98.8%.

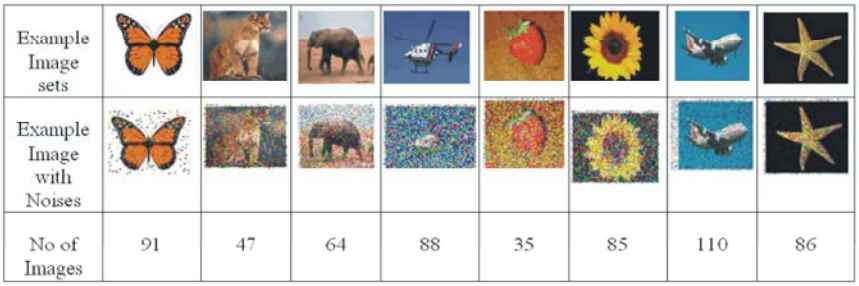

Fig. 3: Caltech 101 database Images

Table 1: Recognition Rate for Query in Different Angles

Image Set		Angle 30°	Angle 60°	Angle 90°	Angle 120°
Classical Image	Set 1	91.5	93.3	**97.8**	94.7
	Set 2	96.4	90.4	88.5	94.5
	Set 3	95.2	92.4	90.9	96.7
	Set 4	89.6	95.3	92.7	88.3
	Set 5	95.6	91.5	97.2	89.9
Texture	Set 6	97.7	88.4	93.7	95.2
	Set 7	96.8	95.2	92.7	94.1
	Set 8	89.5	96.2	93.8	97.1

Table 2: Recognition Rate for Query in Different Scaling Factor

Image Set		Scaling Factor 30x30	Scaling Factor 60x60	Scaling Factor 90x90
Classical Image	Set 1	95.4	91.5	98.1
	Set 2	93.2	97.5	96.3
	Set 3	97.8	88.3	89.4
	Set 4	96.4	92.8	98.2
	Set 5	97.1	91.3	94.7
Texture	Set 6	**98.3**	95.5	88.9
	Set 7	88.5	96.7	91.9
	Set 8	89.4	87.2	96.2

Table 3: Recognition Rate for Query in Normal

Image Sets	Recognition Rate
Set 1	98.3
Set 2	97.8
Set 3	98.1
Set 4	98.6
Set 5	97.3
Set 6	**98.8**
Set 7	97.4
Set 8	97.8

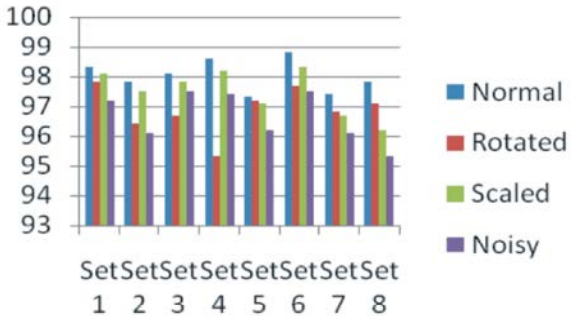

Fig. 5: Recognition Rate for Different Query Types in Different Datasets

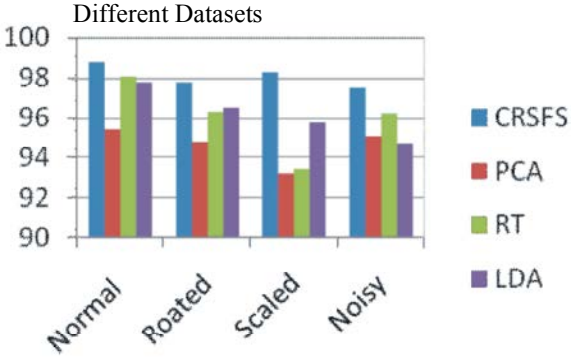

Fig. 6: CRSFS Maximum Recognition Rates is compared with other existing methods like Radon Transform (RT), Linear Discriminant Analysis (LDA) & Principal Component Analysis (PCA).

DISCUSSIONS

Image retrieval completed using our proposed method Combined Radon Space Features Set. This proposed methods recognition rate is compared with the mention literatures & references [2, 4, 6, 9, 10]. This is represent our proposed combined feature space matrix is very effectively represent the image features. From the different situation conducted in different query environments it appears that the performance is improved with the increased number of related images retrieved followed by query image. Table [1-4] represented the different query types used and achieved the better recognition rate.

Table 4: Recognition Rate for Query in Different Noises

Noise Types	CRSFS	PCA	RT	LDA
Salt & Pepper Noise (Variance = 0.05)	98.5	66.9	96.45	94.725
Salt & Pepper Noise (Variance = 0.1)	94.45	64.7	92.538	90.7
Salt & Pepper Noise (Variance = 0.15)	95.25	60.025	96.34	94.725
Salt & Pepper Noise (Variance = 0.2)	85.525	56.775	81.67	76.725
Additive Noise (mean = 0.05, variance =0.05)	91.5	60.2	86.455	84.45
Additive Noise (mean = 0.1, variance =0.1)	68.258	44.75	61.56	55.575
Additive Noise (mean = 0.15, variance =0.15)	46.725	34.375	40.34	43
Additive Noise (mean = 0.2, variance =0.2)	33.58	22.625	30.25	26.95
Uniform Noise (Speckle Variance =0.05)	98.625	68.5	97.5	96.925
Uniform Noise (Speckle Variance =0.1)	97.924	66.125	96.125	94.175
Uniform Noise (Speckle Variance =0.15)	92.350	63.725	89.55	90.2
Uniform Noise (Speckle Variance = 0.2)	86.540	61.575	84.875	83.625

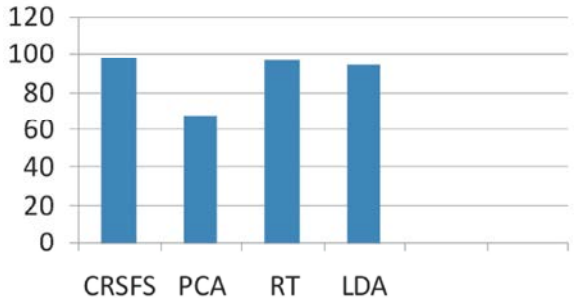

Fig. 7: Performance Comparison of Proposed Method CRSFS, PCA, RT and LDA in salt & pepper noise variance = 0.05.

Table 5: Recognition Rate for L1 & L2 Distance Measures

Image Set		Distance Measures	
		L1	L2
Classical Image	Set 1	0.25	0.87
	Set 2	0.31	0.56
	Set 3	0.18	0.73
	Set 4	0.29	0.66
	Set 5	0.45	0.88
Texture	Set 6	0.13	0.91
	Set 7	0.17	0.93
	Set 8	0.21	0.73

Table [5] represented the two types of distance measure methods L1 & L2 applied in this datasets and distance measures value is point up. Fig [5, 6] represented the proposed method recognition rates was compared with other existing methods. The all above situations Tables [1-4] experiments values is clear to report this proposed method performance is good.

CONCLUSION

Image Retrieval method has been described in this work. The main part of this work is PCA and LDA directly apply to the radon space relatively than images. In this work radon transform used in this method was FFT based. The method was verified Caltech 101 database contains 8 image sets. The best recognition rate 98.8%, 97.8%, 98.3% and 97.5% achieved by normal, rotated, scaled and noisy query environments.

The Enhanced Radon Transform achieved in this method better than related works stated in the literature review section 2.

REFERENCES

1. Michel, S. lew, Nicu Sebe, Chabane Djeraba and Ramesh Jain, 2006. Content-Based Multimedia Information Retrieval: State of the Art and Challenges, ACM Transactions on Multimedia Computing, Communications and Applications, 2(1): 1-19.
2. Ho Young Lee, Ho Keun Lee and Yeong Ho Ha, 2003. Spatial Color Descriptor for Image Retrieval and Video Segmentation, IEEE Transactions on Multimedia, 5(3).
3. Gwénolé Quellec, Mathieu Lamard and Guy Cazuguel, 2010. Adaptive Nonseparable Wavelet Transform via Lifting and its Application to Content-Based Image Retrieval, IEEE Transactions on Image Processing, 19(1).
4. Manesh Kokare, P., K. Biswas and B.N. Chatterji, 2005. Texture Image Retrieval Using New Rotated Complex Wavelet Filters, IEEE Transactions on Systems Man,and Cybernetics—PART B: Cybernetics, 35(6).
5. Hui Hui Wang, Dzulkifli Mohamad and N.A. Ismail, 2013. Semantic Gap in CBIR: Automatic Objects Spatial Relationships Semantic Extraction and Representation, International Journal Of Image Processing (IJIP), 4(3).

6. Te-Wei Chiang and Tien-Wei Tsai, 2006. Content-Based Image Retrieval via the Multiresolution Wavelet Features of Interest, Journal of Information Technology and Applications, 1(3): 205-214.
7. Gwénolé Quellec, Mathieu Lamard and Guy Cazuguel, 2012. Fast Wavelet-Based Image Characterization for Highly Adaptive Image Retrieval, IEEE Transactions on Image processsing, 21(4).
8. Yue Gao, Meng Wang, Zheng-Jun Zha, Jialie Shen, Xuelong Li and Xindong Wu, 2013. Visual-Textual Joint Relevance Learning for Tag-Based Social Image Search, IEEE Transations on image processing, 22(1).
9. Qianni Zhang and Ebroul Izquierdo, 2013. Histology Image Retrieval in Optimized Multifeature Spaces, IEEE Journal of Biomedical and Health informatics, 17(1).
10. Kekre, H.B. and Dhirendra Mishra, 2011. Content Based Image Retrieval Using Full Haar Sectorization, International Journal of Image Processing (IJIP), 5(1).
11. Yi-Chen Chen, Challa S. Sastry, Vishal M. Patel, P. Jonathon Phillips and Rama Chellappa, 2013. In-Plane Rotation and Scale Invariant Clustering Using Dictionaries, IEEE Transactions on Image Processing, 22(6).
12. Andrew P. Papli´nski, 2010. Rotation Invariant Categorization of Visual Objects Using Radon Transform and Self-Organizing Modules, ICONIP 2010, Part II, LNCS, 6444: 360-366.
13. Andrew P. Papli´nski, 2012. Rotation-Invariant Categorization of Colour Images using the Radon Transform, WCCI 2012 IEEE World Congress on Computational Intelligence, Brisbane, Australia.
14. Hamid M. Hasan, Waleed A. AL.Jouhar and Majid A. Alwan, 2012. Face Recognition Using Improved FFT Based Radon by PSO and PCA Techniques, International Journal of Image Processing (IJIP), 6(1).
15. Kourosh Jafari-Khouzani and Hamid Soltanian-Zadeh, 2005. Rotation Invariant Multiresolution Texture Analysis Using Radon and Wavelet Transforms, IEEE Trans Image Process. 2005 June, 14(6): 783-795.
16. Ahmed Q. AL-Thahab, 2012. Image Recognition Using Combination of Multiwavelet and Radon Transforms with Neural Network, Journal of Babylon University/Engineering Sciences, 20(1).
17. Image Noise, http://en.wikipedia.org/wiki/ Imagenoise
18. NoiseModels, http://homepages.inf.ed.ac.uk/ rbf/ Cvonline/ LOCAL_COPIES/ VELDHUIZEN/ node11.html
19. Xiaorong Pu, Zhang YI and Zhongjie Fang, 2008. Holistic and partial facial features futions by binary particle swarm optimization, Neural Comput & Applic, 17: 481-488.
20. Belhumeur, P.N., J.P. Hespanala and D.J. Kriegman, 1997. Eigenfaces vs. fisherfaces: recognition using class specific linear projection. IEEE Trans Pattern Anal Mach Intell, 19(7): 711-720.
21. Ruba Soundar Kathavarayan and Murugesan Karuppasamy, 2010. Preserving Global and Local Features for Robust Face Recognition under Various Noisy Environments, International Journal of Image Processing (IJIP) 3(6).
22. Belhumeur, P.N., J.P. Hespanha and D.J. Kriegman, 1997. Eigenfaces vs. Fisherfaces: recognitionusing class specific linear projection, IEEE Transactions on Pattern Analysis and Machine Intelligence, 19(7): 711-720.
23. Zolghadri-Jahomi, M. and M.R. Valizadeh, 2006. A Proposed Query -Sensitive Similarity Measure, Iranian Journal of Science & Technology, 30(B2).
24. Al-Khaffaf, H.S.M., A.Z. Talib and R. Abdul Salam, 2009. A Study on the effects of noise level, cleaning method and vectorization software on the quality of vector data, Lecture Notes in Computer Science, pp: 299-309.